DOE/NASA/12726-17
NASA TM-82913

Chemical and Electrochemical Behavior of the Cr(III)/Cr(II) Half Cell in the NASA Redox Energy Storage System

David A. Johnson
Spring Arbor College

and

Margaret A. Reid
National Aeronautics and Space Administration
Lewis Research Center

Work performed for
U.S. DEPARTMENT OF ENERGY
Conservation and Renewable Energy
Division of Energy Storage Systems

Prepared for
162nd Meeting of the Electrochemical Society
Detroit, Michigan, October 17–22, 1982

DOE/NASA/12726-17
NASA TM-82913

Chemical and Electrochemical Behavior of the Cr(III)/Cr(II) Half Cell in the NASA Redox Energy Storage System

David A. Johnson
Spring Arbor College
Spring Arbor, Michigan 49283

and

Margaret A. Reid
National Aeronautics and Space Administration
Lewis Research Center
Cleveland, Ohio 44135

Work performed for
U.S. DEPARTMENT OF ENERGY
Conservation and Renewable Energy
Division of Energy Storage Systems
Washington, D.C. 20545
Under Interagency Agreement DE-AI04-80AL12726

Prepared for
162nd Meeting of the Electrochemical Society
Detroit, Michigan, October 17–22, 1982

CHEMICAL AND ELECTROCHEMICAL BEHAVIOR OF THE Cr(III)/Cr(II) HALF CELL IN THE NASA REDOX ENERGY STORAGE SYSTEM*

David A. Johnson
Department of Chemistry
Spring Arbor College
Spring Arbor, Michigan 49283

Margaret A. Reid
National Aeronautics and Space Administration
Lewis Research Center
Cleveland, Ohio 44135

ABSTRACT

The Cr(III) complexes in the NASA Redox Energy Storage System have been isolated and identified as $Cr(H_2O)_6^{+3}$ and $Cr(H_2O)_5Cl^{+2}$ by ion-exchange chromatography and visible spectrophotometry. The cell reactions during charge-discharge cycles have been followed by means of visible spectrophotometry. The spectral bands were resolved into component peaks and concentrations calculated using Beer's Law. During the charge mode $Cr(H_2O)_5Cl^{+2}$ is reduced to $Cr(H_2O)_5Cl^{+}$ and during the discharge mode $Cr(H_2O)_5Cl^{+}$ is oxidized back to $Cr(H_2O)_5Cl^{+2}$. Both electrode reactions occur via a chloride-bridge inner-sphere reaction pathway. Hysteresis effects can be explained by the slow attainment of equilibrium between $Cr(H_2O)_6^{+3}$ and $Cr(H_2O)_5Cl^{+2}$.

E-1318

INTRODUCTION

The NASA Redox Energy Storage System is an electrochemical storage device that utilizes the oxidation and reduction of two soluble redox couples for

---

*Work funded by the U. S. Department of Energy under Interagency Agreement DE-A104-80AL12726.

charging and discharging. The active electrode materials, separated by a highly selective ion exchange membrane, are pumped through a stack of Redox flow cells where the electrochemical reactions take place at porous carbon felt electrodes. The redox couples currently used are acidified solutions of chromium [Cr(III)/Cr(II)] and iron [Fe(III)/Fe(II)].

The Redox technology has matured from the conceptual stage (1) to the present status of actual working systems with predictable performance, high reliability, stable operation, and long life (2). Applications for this technology include stand-alone power systems using solar photovoltaic or wind energy as the primary energy source and in electric utility service where load-leveling capacity is required.

A schematic diagram of a single Redox cell and the electrode reactions is shown in Fig. 1. An anion-exchange membrane separates the compartments and prevents the cross-mixing of the reactive cations. Electrodes consist of carbon felt, catalyzed on the chromium side by trace amounts of gold and lead. The catalyst is required on the chromium side because the rate of reduction of Cr(III) to Cr(II) is slow on most surfaces (3 and 4). The catalyst must also have a high overvoltage for hydrogen since, from a thermodynamic standpoint, hydrogen is evolved before chromium is reduced. Appreciable coevolution of hydrogen reduces coulombic efficiency and allows the system to get out of balance electrochemically after many cycles. Trace amounts of gold (12 to 25 ug/cm^2) and lead (100 to 200 ug/cm^2) deposited on the carbon felt meet the requirements for an effective catalyst (5). Trace amounts of gold seem to be necessary to produce a surface on which lead deposits uniformly during the charging cycle. The catalyst also improves the cell discharge rate (6). No catalyst is required to the iron side.

During discharge, chloride ions move from the cathode compartment to the anode compartment, and hydrogen ions move in the opposite direction. On charge all reactions are reversed. Since all species are fully soluble, there are no life-limiting factors such as shape changes, inactive forms of reactants, and dendrite formation. There are also many advantages in system sizing and control that have been discussed elsewhere (2 and 7).

Semipermeable membranes have been developed that are sufficiently conductive and selective for use for photovoltaic and wind energy storage applications (8). Methods of keeping the system in balance have been developed. Flow characterization and analysis of shunt currents have been carried out, and hardware has been scaled up with little difficulty (9).

The relatively inert inner-sphere complex ions $Cr(H_2O)_5Cl^{+2}$ and $Cr(H_2O)_4Cl_2^{+}$ are present at equilibrium with $Cr(H_2O)_6^{+3}$ in aqueous solutions containing Cr(III) and chloride ion (10). The presence of these complex ions is evidenced by both color changes and open-circuit voltage versus state-of-charge plots. Distinctive differences in the chromium solutions are observed at the same state of charge depending on whether the cell is in the charge or discharge mode (11). The open-circuit voltage behavior is shown in Fig. 2, in which the open-circuit voltages during charge and discharge modes are plotted as a function of state-of-charge for a complete cycle. In addition, above 50 percent state-of-charge, the charging rate drops off appreciably.

Since these effects contribute to lower energy storage efficiency it was critical to undertake a thorough study of the processes occurring at the chromium electrode during the charging and discharging of the system.

This paper describes the results of spectrophotometric studies and measurements of electrode potential of the chromium solutions during complete charge-discharge cycles of a single subscale Redox cell.

EXPERIMENTAL

The laboratory subscale flow cell has been described previously (2 and 7). A standard Redox membrane (CDIL series) supplied by Ionics of Watertown, Massachusetts was used in the cell. Electrodes were made from nominally 1/8 in. carbon felt. The electrode on the iron side was uncatalyzed while the electrode on the chromium side was treated and loaded with gold and lead as previously described (6). One set of experiments was carried out using 1 M $CrCl_3$ and $FeCl_2$ solutions in 2 M HCl; the other set with 0.45 M $CrCl_3$ and 0.55 M $FeCl_2$ so that the absorbance would be less than 2.0 for all states of charge.

A 1 mm quartz flow cell was connected in parallel hydraulically with the chromium side of the Redox cell and placed in a Beckman DK-2A Spectrophotometer. The spectrum was then recorded at selected states of charge from 350 to 1000 nm. The complexes $Cr(H_2O)_6^{+3}$, $Cr(H_2O)_5Cl^{+2}$ and $Cr(H_2O)_4Cl_2^{+}$ were prepared according to procedures developed by Angelici using ACS certified chemicals and deionized water (11). The spectra were recorded and agreed with literature reports (12) (Fig. 3). Solutions of $Cr(H_2O)_6^{+3}$ and $Cr(H_2O)_5Cl^{+2}$ in 1 M $HClO_4$ follow Beer's Law up to 0.70 M and 0.40 M respectively, which are the highest concentrations obtained in solutions from the ion exchange column so far.

Cr(II) was prepared according to a method used by Myers and Taube (13). First $Cr(H_2O)_6^{+2}$ was prepared by reducing $Cr(ClO_4)_3$ in 1.0 M $HClO_4$ with amalgamated zinc. The solution was protected from atmospheric oxygen by a stream of dry nitrogen. The spectrum was obtained using a 1 mm quartz flow cell. It was necessary to use a flow cell because of the rapid oxidation of Cr(II) in air. The absorption maxima was at 714 nm, identical to that reported in the literature (14). Cr(II) was also prepared by reducing

$CrCl_3 \cdot 6H_2O$ in 6.0 M HCl. The absorption maxima was at 750 nm. Reduction of $CrCl_3 \cdot 6H_2O$ in lower concentrations of HCl gave maximum absorption peaks between 714 and 750 nm.

The Cr(III) species present in the uncharged cell solution were identified by ion-exchange chromatography. Approximately 10 ml of cell solution was placed on a column of Dowex 50X8-100 cation exchange resin (50-100 mesh H^+ form). The sample was eluted with 0.1 M, 1.0 M and 3.0 M $HClO_4$, respectively, and spectra of the resulting fractions recorded. Maxima of the first two fractions occurred at 430 and 605 nm, characteristic of $Cr(H_2O)_5Cl^{+2}$ (12 and 15). The spectrum of the third portion was identical to that of the $Cr(H_2O)_6^{+3}$. The cell solution was analyzed prior to a charge-discharge cycle and after two complete cycles. The absorption maxima were identical in each case.

The spectra measured during the charge and discharge cycles were analyzed using a Du Pont 310 Curve Resolver. The procedure was to start the resolving process first by considering the spectra of the highest charged solution. The solution consisted mainly of $Cr(H_2O)_6^{+3}$ and Cr(II) as indicated by absorption maxima. Once the curves due to $Cr(H_2O)_6^{+3}$ and Cr(II) were established it was not difficult to adjust the curves for other states-of-charge and add the contribution of $Cr(H_2O)_5Cl^{+2}$. The relative absorbances of the two peaks of the Cr(III) species were always kept in the ratio of the molar absorptivities (12). The concentrations of the Cr(III) species were then calculated from the resolved curves using Beer's Law. Half-cell electrode potentials were measured with a wax-filled graphite rod against a Ag/AgCl (4 M KCl) reference electrode in the electrolyte reservoir.

RESULTS AND DISCUSSION

The spectra obtained from the chromium solutions of the redox cell were characterized by two broad absorption bands with maxima of 408 to 430 nm and

575 to 610 nm. In the highly charged state a band with a maximum at 750 nm was also observed. Fig. 4 is a typical spectra.

Since the maxima fell within the limits of the absorption maxima of $Cr(H_2O)_6^{+3}$ and $Cr(H_2O)_5Cl^{+2}$ it seemed appropriate to begin the work by isolating and identifying those ions which might be present at equilibrium in acidified Cr(III) chloride cell solutions.

The cell solution was analyzed prior to and immediately after taking it through two complete charge-discharge cycles using ion-exchange chromatography and spectrophotometry. The results indicated that only $Cr(H_2O)_6^{+3}$ and $Cr(H_2O)_5Cl^{+2}$ were present in completely discharged solutions in detectable amounts under normal operating conditions of the cell. According to the equilibrium constants reported in the literature, $Cr(H_2O)_5Cl^{+2}$ and $Cr(H_2O)_6^{+3}$ should be the dominant existing species once equilibrium has been achieved (16 and 17). This means that consideration need only be given to the spectral contributions from $Cr(H_2O)_6^{+3}$ and $Cr(H_2O)_5Cl^{+2}$, and any contribution from $Cr(H_2O)_4Cl_2^{+}$ can be neglected. An attempt to include spectral contributions of $Cr(H_2O)_4Cl_2^{+}$ in the resolving process also proved to be unnecessary in agreement with the results from analysis using ion-exchange chromatography.

The band with a maximum at 750 nm is obviously due to the presence of Cr(II). Since the only literature value located for Cr(II) was 714 nm, it was necessary to determine the exact contribution of Cr(II) to the observed spectra. $Cr(H_2O)_6^{+2}$ has been prepared and identified as having a maximum at 714 nm (14). $Cr(H_2O)_6^{+2}$ was prepared and one absorption maxima at 715 nm was identified. Since Cr(II) is a d^4 system, its absorption spectra is expected to be strongly influenced by the Jahn-Teller Effect. The absorption peak at 715 nm tails off at the longer wavelengths, indicating the

presence of the Jahn-Teller Effect. The preparation of Cr(II) in an environment containing the ligand, chloride ion in varying concentrations, shows a shift in the maximum to longer wavelengths. This indicates that the ligand field strength has decreased and is strong evidence for the formation of a new complex ion where at least one water molecule has been replaced by a chloride ion. According to the spectrochemical series, chloride ion does not have as great a capacity to split the d orbitals as does water, reflecting decreased ligand field strength (18). The fact that the maximum wavelength varies with chloride concentration and reaches a maximum at 750 nm suggests then that Cr(II) exists in aqueous solutions as several complex ions. Since $Cr(H_2O)_6^{+2}$ has been identified with an absorption maximum at 714 nm, it seems reasonable that $Cr(H_2O)_5Cl^{+}$ might be another species present with an absorption maximum at 750 nm. This speculation is further supported by mechanistic studies which will be discussed in detail later (4).

In each run, the cell was taken through two complete charge-discharge cycles. At selected states-of-charge the open-circuit voltage and spectra of the chromium solutions were recorded. The results of the second run with 0.55 M $FeCl_2$ and 0.45 M $CrCl_3$ in 2.0 M HCl are presented in Figs. 5 and 6. The results from the first run in which the solutions were 1.0 M $FeCl_2$ and 1 M $CrCl_3$ each in 2.0 M HCl are similar.

Figures 5 and 6 show the concentrations of $Cr(H_2O)_6^{+3}$ and $Cr(H_2O)_5Cl^{+2}$ at selected states-of-charge and -discharge. The error in the measurements is believed to be less than 2 percent. Differences between the two cycles are due to the different ratios of the species in the initial solutions and the different modes of cycling. The important features of both Figs. are the large decrease in $Cr(H_2O)_5Cl^{+2}$ concentration with increasing state-of-charge and the rather small change in $Cr(H_2O)_6^{+3}$

concentration with increasing state-of-charge. It is significant to note that whereas the $Cr(H_2O)_5Cl^{+2}$ concentration decreases to a minimal value at high states-of-charge, the $Cr(H_2O)_6^{+3}$ concentration remains relatively high compared to its initial concentration. This is strong evidence that $Cr(H_2O)_5Cl^{+2}$ is the predominant species involved in the reduction reaction at the electrode surface. Weaver and Anson have carried out extensive studies of the electrode reactions of $Cr(H_2O)_5X^{+2}$ complexes at mercury electrodes and have found electrode reaction rate constants of 2.2×10^{-5} and 5.60×10^{-3} for $Cr(H_2O)_6^{+3}$ and $Cr(H_2O)_5Cl^{+2}$ respectively, evaluated at -700 mV versus SCE (4). In addition they were able to determine that the reduction of $Cr(H_2O)_5Cl^{+2}$ follows a chloride-bridged inner-sphere electrode reaction mechanism by the decrease in rate with the addition of the strongly absorbed but chemically inactive iodide ion and the greater potential dependence of the reaction rate. Although the surface of the catalyzed carbon felt electrode is quite different from the surface of mercury, the relative activity of the two species is similar. This is strong evidence that the reduction of $Cr(H_2O)_5Cl^{+2}$ proceeds by a chloride-bridged inner-sphere mechanism on the catalyzed carbon felt surface. Likewise the relatively small change in the $Cr(H_2O)_6^{+3}$ concentrations suggests that it is not directly involved in the electrode reaction and can be explained on the basis of a slowly achieved equilibrium state between the hexa- and pentahydrate.

During discharge, Figs. 5 and 6 show a rapid rise in the $Cr(H_2O)_5Cl^{+2}$ concentration as discharge continues. There is relatively little change in the $Cr(H_2O)_6^{+3}$ concentration until the $Cr(H_2O)_5Cl^{+2}$ concentration increases appreciably. This suggests that the oxidation process involves the production of $Cr(H_2O)_5Cl^{+2}$ rather than $Cr(H_2O)_6^{+3}$. In addition, the fact that the $Cr(H_2O)_6^{+3}$ concentration changes only after $Cr(H_2O)_5Cl^{+2}$

concentration has reached an appreciable level suggests an equilibrium step involving $Cr(H_2O)_6^{+3}$ and $Cr(H_2O)_5Cl^{+2}$. This is in agreement with Gates and King who have studied the equilibrium quotient for the reaction $Cr(H_2O)_6^{+3} + Cl^- = Cr(H_2O)_5Cl^{+2} + H_2O$ to be 0.27 at 30°C (10). (The equilibrium quotient is similar to the equilibrium constant, but concentrations are used instead of activities. In this work the ionic strength was held constant at 4.0). The equilibrium state is achieved very slowly in the absence of Cr(II) ion. There is evidence that the rate of aquation of $Cr(H_2O)_5Cl^{+2}$ to form $Cr(H_2O)_6^{+3}$ is catalyzed by Cr(II) ion (19 and 20).The differences in concentrations of the hexa- and pentahydrate at the same state of charge for the first and second charges can be explained on the basis of this slow equilibration of the species. The original solution had been prepared from the solid relatively recently and presumably had a higher proportion of pentahydrate than the equilibrium concentration.

The electrode potentials in the chromium solution with respect to a Ag/AgCl reference electrode are plotted in Fig. 7 against the log of the ratio of concentration of Cr(II) to the concentrations of the different Cr(III) species. It can be seen that the curve for the pentahydrate species is linear and has a slope close to the Nernst slope, whereas the curves for the total Cr(III) concentration and the hexahydrate are not. This Nernstian behavior, together with the formation of $Cr(H_2O)_5Cl^{+2}$ in the discharge mode and the disappearance of $Cr(H_2O)_5Cl^{+2}$ in the charge mode along with the spectra of the Cr(II) species is strong evidence that $Cr(H_2O)_5Cl^{+}$ is the predominant Cr(II) species involved in the electrode reaction. Weaver and Anson have found that the oxidation of Cr(II) takes place by means of a chloride-bridged inner-sphere pathway at a mercury electrode. They suggest that a more efficient reaction pathway is provided by the presence of chloride ion (4).

The Frank-Condon principle points out that the motions of heavy atoms are negligibly slow with respect to the rapid motions of electrons. During those rearrangements which constitute a reaction, the electronic state of the system is determined by atomic geometry. For each redox reaction there exists a specific atomic arrangement equidistant from product and reactant, at which oxidation or reduction is consumated. This requirement constitutes a considerable barrier to reaction if the reduced and oxidized forms differ greatly in atomic geometry and if rearrangement between the two forms involves a large activation energy (3). Consequently one would expect $Cr(H_2O)_5Cl^{+2}$ to retain atomic geometry upon reduction and the Cr(II) species to retain atomic geometry upon oxidation. This means that the reaction pathway will most likely involve $Cr(H_2O)_5Cl^{+2}$ and $Cr(H_2O)_5Cl^{+}$ for both the reduction and the oxidation reactions. The experimental evidence is clearly supportive of this reaction pathway both at a mercury electrode and a catalyzed carbon electrode (4).

Products of redox reactions involving aquachromium (II) differ somewhat in geometry from Cr(III). Aquachromium (II) ion is a d^4 system and is considered to resemble aquacopper (II) ion. It is subject to severe Jahn-Teller distortions as previously mentioned. Distortion of Cr(III) towards the Cr(II) structure therefore must overcome the crystal field stabilization of octahedral Cr(III). Slow rates for the reduction of Cr(III) are therefore to be expected and indeed have been demonstrated (3). Thus, the reduction of $Cr(H_2O)_5Cl^{+2}$ would be expected to be slow since the spectra of $Cr(H_2O)_5Cl^{+}$ gives strong indication of Jahn-Teller distortions. However in this case the effect of surface reactions must be considered (3). Certain isothiocyanate complexes which are strongly absorbed on the surface of mercury electrodes by means of mercury-sulfur bonds have been shown to undergo reduc-

tion via the faster inner-sphere electrode reactions (21 to 23). Likewise specific absorption at the aqueous-mercury interface of anions also increases the probability of the faster inner-sphere mechanism (23 and 24).

During electrode reactions which proceed by inner-sphere pathways, one or more of the ligands in the reactant's primary coordination sphere penetrates the layer of solvent molecules and ions specifically coordinated to the electrode surface (4). Thus an inner-sphere chloride-bridged pathway has the effect of providing a more efficient reaction pathway for reduction of $Cr(H_2O)_5Cl^{+2}$ to occur. This more efficient pathway enables the crystal field stabilization of the octahedral $Cr(H_2O)_5Cl^{+2}$ to be overcome and a reasonable rate of reduction to occur.

CONCLUSIONS

We have been able to isolate and identify by ion exchange chromatography and visible spectrophotometry $Cr(H_2O)_6^{+3}$ and $Cr(H_2O)_5Cl^{+2}$ solutions of the discharged NASA Redox Energy Storage System. The reactions at the catalyzed carbon felt electrode can be followed spectrophotometrically during charge-discharge cycles. The spectra can be resolved and used to determine the concentrations of $Cr(H_2O)_6^{+3}$ and $Cr(H_2O)_5Cl^{+2}$ which have been demonstrated to follow Beer's Law up to 0.7 and 0.4 M respectively.

The spectral data indicates that the concentration of $Cr(H_2O)_5Cl^{+2}$ decreases much more rapidly with increasing state of charge than does the concentration of $Cr(H_2O)_6^{+3}$ indicating that $Cr(H_2O)_5Cl^{+2}$ is the predominant species being reduced during the charging cycle. There is a rapid rise in $Cr(H_2O)_5Cl^{+2}$ concentration as discharge takes place, and the concentration of $Cr(H_2O)_6^{+3}$ rises only after appreciable $Cr(H_2O)_5Cl^{+2}$ is produced. The electrode potentials also indicate that the chief electroactive species is the pentahydrate.

The results can be interpreted best as the reduction of $Cr(H_2O)_5Cl^{+2}$ via an inner-sphere chloride-bridged electrode reaction and the oxidation of $Cr(H_2O)_5Cl^{+}$ as an inner-sphere chloride-bridged electrode reaction. In addition a slowly attained equilibrium exists between $Cr(H_2O)_6^{+3}$ and $Cr(H_2O)_5Cl^{+2}$ that is catalyzed by Cr(II). The conclusions are in excellent agreement with the results obtained at mercury electrodes.

REFERENCES

1. L. H. Thaller, "Electrically Rechargeable Redox Flow Cells," NASA TM X-71540 (1974).
2. L. H. Thaller, "Recent Advances in Redox Flow Cell Storage Systems," Dept. of Energy, Washington, DC, DOE/NASA/1002-79/4; National Aeronautics and Space Admin., Washington, DC, NASA TM-79186 (1979).
3. J.E. Earley and R.D. Cannon, Transition Metal Chem. 1, 33-109 (1965)
4. M. J. Weaver and F. C. Anson, Inorg. Chem. 15 (8), 1871-1881 (1976).
5. J. Giner and K. Cahill, "Advanced Screening of Electrode Couples," Dept. of Energy, Washington, DC, DOE/NASA/0794-80/1; National Aeronautics and Space Admin., Washington, DC, NASA CR-159738 (1979).
6. M. A. Reid, R. F. Gahn, J. S. Ling, and J. Charleston, "Preparation and Characterization of Electrodes for the NASA-Redox Storage System," Dept. of Energy, Washington, DC, DOE/NASA/12726-13; National Aeronautics and Space Admin., Washington, DC, NASA TM-82702 (1980).
7. L. H. Thaller, "Redox Flow Cell Energy Storage Systems," Dept. of Energy, Washington, DC, DOE/NASA/1002-79/3; National Aeronautics and Space Admin., Washington, DC, NASA TM-79143 (1979).
8. S. A. Alexander, R. B. Hodgdon, and W. A. Waite, "Anion Permselective Membrane," Dept. of Energy, Washington, DC, DOE/NASA/0001-79/1; National Aeronautics and Space Admin., Washington, DC, NASA CR-159599 (1979).

9. J. C. Acevedo, N. H. Hagedorn, P. R. Prokopius, and L. H. Thaller, "Shunt Current Modeling of Redox Stacks," Extended Abstracts of the 156th Fall Meeting of the Electrochemical Society, (Electrochemical Society, Inc., New Jersey, 1979), Vol. 79-2, Abstract No. 170, pp. 446-448.

10. H. S. Gates and E. L. King, J. Am. Chem. Soc., 80 (19) 5011-5015 (1958).

11. Robert Angelici, Synthesis and Technique in Inorganic Chemistry (W. B. Saunders, Philadelphia, 1968).

12. P. J. Elving and B. Zemel, J. Am. Chem. Soc. 79 (6), 1281-1285 (1957).

13. H. Taube and H. Myers, J. Am. Chem. Soc. 76 (8), 2103-2111 (1954).

14. O. G. Holmes and D. S. McClure, J. Chem. Phys., 26 (6), 1686-1694 (1957).

15. T. W. Swaddle and E. L. King, Inorg. Chem. 4(4), 532-538 (1965).

16. M. Magini, J. Chem. Phys. 73(5), 2499-2505 (1980).

17. L. G. Sillen and A. E. Martell, "Stability Constants of Metal-ion Complexes," Chem. Soc. Spec. Publ. No. 17 (1964).

18. F. A. Cotton and G. Wilkinson, Advanced Inorganic Chemistry, (Interscience Publishers, New York, 1972), 3rd ed.

19. D. L. Ball and E. L. King, J. Am. Chem. Soc. 80 (5), 1091-1094 (1958).

20. A. Adin and A. G. Sykes, J. Chem. Soc. A 1518-1521 (1966).

21. F. C. Anson and R. S. Rodgers, J. Electroanal. Chem. 47, 287-309 (1973).

22. M. J. Weaver and F. C. Anson, J. Electroanal Chem. 58, 95-121 (1975).

23. M. J. Weaver and F. C. Anson, J. Am Chem. Soc. 97 (15), 4403-4405 (1975).

24. D. A. Aikens and J. W. Ross, J. Phys. Chem. 65 (7), 1213-1216 (1961).

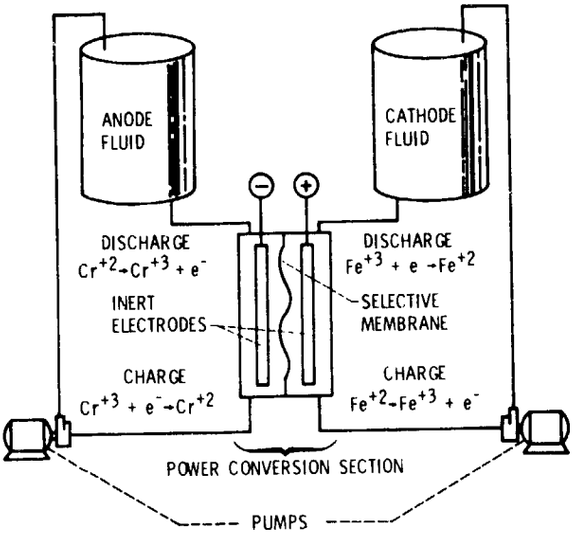

Figure 1. - Principle of operation of NASA-Redox concept.

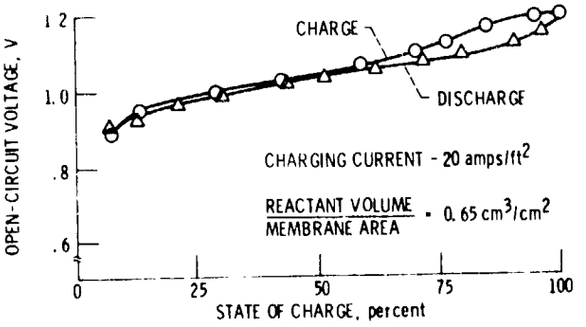

Figure 2. - Open-circuit voltage hysteresis of iron/chromium Redox cell

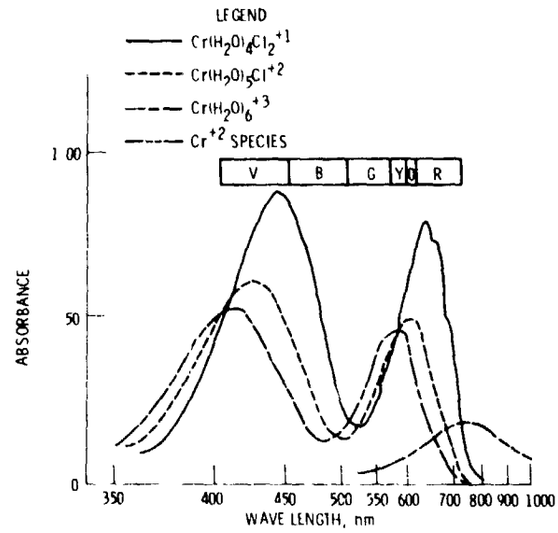

Figure 3 - Spectra of chromium complex ions

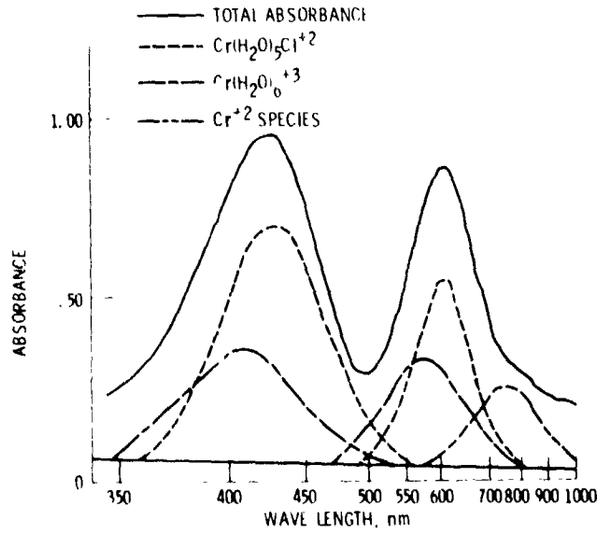

Figure 4 - Spectrum of chromium Redox solution during discharge (42.0 % CHARGED, 58.0 % DISCHARGED).

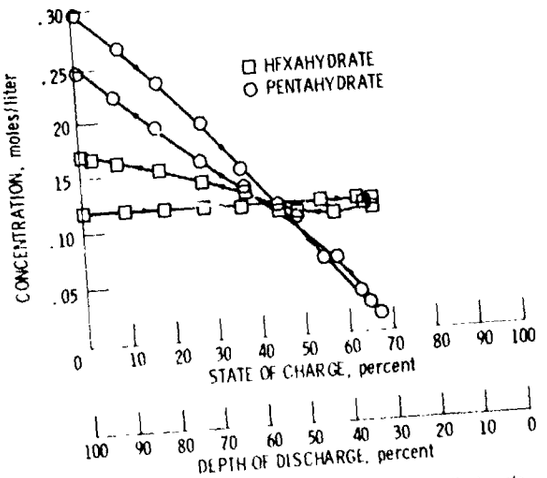

Figure 5. Concentrations of Cr(III) species first cycle, taper current charge

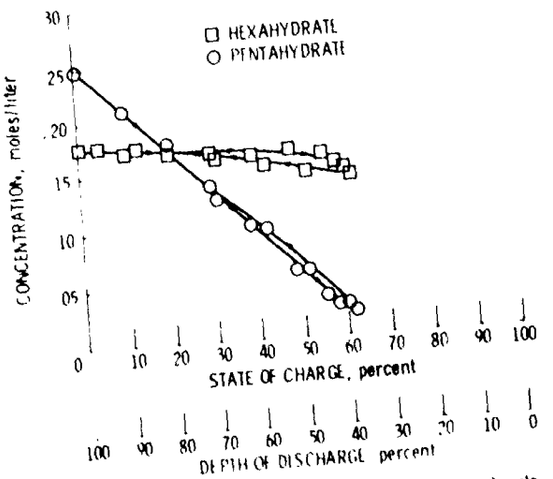

Figure 6. Concentrations of Cr(III) species second cycle, constant current charge, 20 ASF

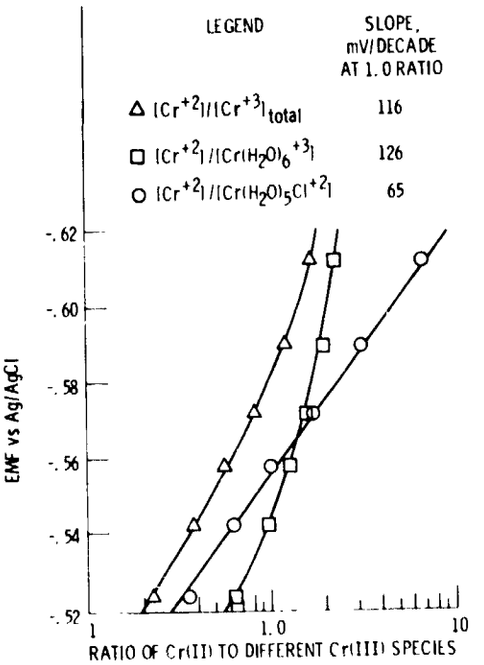

Figure 7 - Test of Nernst equation in chromium Redox solutions. First charge (varying current).